DRAL
Daresbury Laboratory
Rutherford Appleton Laboratory

RAL Report
RAL-95-006

Future Opportunities and Present Possibilities for Coherent Inelastic Single Crystal Measurements on Pulsed Neutron Sources

M Hagan, U Steigenberger, C Petrillo and F Sacchetti

January 1995

Rutherford Appleton Laboratory Chilton DIDCOT Oxfordshire OX11 0QX

Future opportunities and present possibilities for coherent inelastic single crystal measurements on pulsed neutron sources

M Hagen
Department of Physics, Keele University, Keele, Staffordshire ST5 5BG, U.K.

U Steigenberger
ISIS Facility, Rutherford Appleton Laboratory, Chilton, Didcot, Oxon OX11 0QX, UK

and

C Petrillo and F Sacchetti
Dipartimento di Fisica, Universitá di Perugia, Via A.Pascoli, I-06100 Perugia, Italy
and
Istituto di Struttura della Materia del Consiglio Nazionale delle Ricerche,
Via E.Fermi 38, I-00044 Frascati, Italy

Abstract

The triple axis spectrometer (TAS) has long been the mainstay for measuring excitations in single crystal samples. In a recent paper Dorner has claimed that the TAS would be the instrument of choice for such measurements at any future high flux spallation neutron source. However, a comparison of the operational characteristics of a TAS and those of direct and indirect geometry time of flight spectrometers for this type of measurement at a pulsed source shows that the TAS would not in fact be a particularly competitive instrument for this purpose.

1 Introduction

Inelastic neutron scattering is an unrivalled technique for probing the wavevector and energy dependence of structural and magnetic excitations in solids. In order to obtain the full wavevector dependence of the excitations in crystalline materials it is essential to work with single crystal specimens. In a recent paper Dorner [1] discussed whether measurements of S(**Q**,E) in single crystal samples are more effectively carried out by a triple axis spectrometer (TAS) or by time of flight (ToF) techniques. He concluded that the TAS was the superior instrument and that it would remain the preferred instrument for these types of measurement for any future high flux spallation neutron source, including the proposed European Spallation Source (ESS) [2], which will have a time integrated neutron flux comparable to that of the ILL, but with a sharp pulse structure. Dorner's assertion was based on the argument that when measuring phonon dispersion curves it was necessary to determine the eigenvector of the phonon mode as well as its energy. This can only be done by performing constant-Q scans at specific points in reciprocal space and therefore Dorner concluded that this required the use of a TAS.

This conclusion contains a simple flaw, which is to assume that a constant-Q scan and the use of a TAS instrument are synonymous - **they are not**. The wavevector **Q** and energy transfer E in a neutron scattering experiment are given through the incident ($\mathbf{k}_i$) and scattered ($\mathbf{k}_f$) wavevectors of the neutron. These wavevectors can be equally well defined by time of flight techniques as they can be by Bragg reflection from a crystal. Hence a constant-Q scan can be just as well performed with a ToF instrument as it can be with a TAS. In the past the ToF technique has not been used because of flux limitations. The pulsed beam of a steady state reactor and the time averaged flux of present day spallation sources are too low to carry out a competitive constant-Q scan. A **pulsed high flux** source like the ESS will change this situation entirely and a constant-Q scan could be equally well performed with ToF techniques.

The question of what instrumentation would be appropriate for any future high flux spallation source is therefore not simply a question of whether a "phonon spectrometer" can perform constant-Q scans to isolate phonon eigenvectors, but whether the instrumentation can provide **additional** new information or information at a greater data rate without, of course, giving up the capacity to do what can be done today. Although, as was noted by Dorner [1], a TAS operating at an ESS type source would have advantages over a TAS operating at a present day high flux reactor, these are small compared to the scope for new opportunities which are provided by using ToF techniques.

There are many questions which arise from this simple observation. Which ToF techniques are the most suitable ? What sort of instrument development work is required ? Can the instrumentation which is already available at present day spallation sources be used profitably *now* rather than waiting for an ESS type source ? In this paper we present a view of the wider possibilities for instrumentation at a high flux pulsed source and some of the future scientific opportunities in single crystal studies. In section 2 we compare the operating characteristics of a TAS with different ToF instruments and discuss the performance of a constant-Q scan using either technique. We describe a conceptual design for a simple, but highly flexible, time of flight instrument for inelastic single crystal measurements at a next generation pulsed neutron source which could provide not only the constant-Q capability, but also new modes of operation not possible with a TAS. In section 3 we discuss optimized measuring methods for different scientific applications and the opportunities for new measuring techniques and sample environment equipment made possible by the pulsed nature of the neutron beam at a spallation source. In section 4 we return to the present and describe what instrumentation is already available at present spallation sources and demonstrate how a continuing development programme is opening up more scientific opportunities. Although the discussion will concentrate on the PRISMA spectrometer at the ISIS Facility, other instruments will also be briefly reviewed. Section 5 contains a summary of the paper.

2 Operational Characteristics of TAS and ToF Spectrometers

2.1 The Triple Axis Spectrometer

A schematic diagram of a TAS is shown in figure (1a). The monochromator crystal uses Bragg reflection to select a single incident neutron energy out of the white beam from the source. This mono-energetic neutron beam is then scattered from the sample and neutrons of a single final energy, at a single scattering angle ϕ, are Bragg reflected by an analyzer crystal into the detector. An appropriate choice of the monochromator, sample, scattering and analyzer/detector angles then allows the TAS to measure the intensity at a single point in (**Q**, E) space. The intensities at a sequence of (**Q**, E) points are measured in a **step by step mode** and features (eg. phonons) are identified by intensity peaks in the scan. In general, the scan direction in (**Q**, E) space can follow any path within the limits of the kinematic constraints on the neutron scattering process. However, the most commonly performed scan is the "constant-Q" scan, where the wavevector transfer **Q** is kept fixed, while the intensity is measured for various energy transfers E. This is shown schematically in the (**Q**,E) diagram of figure (2) by

the sequence of crosses. A TAS at a high flux pulsed neutron source would be used in much the same way as that described above for a reactor based instrument. There is an advantage [1] in operating a TAS at a high flux pulsed source rather than at a high flux reactor source. The monochromator crystal produces "huigher order contamination" i.e. it reflects neutrons of wavelength λ/n as well as those of wavelength λ. At a reactor source the rejection of this contaminant scattering is performed by using a filter. This restricts the choice of either the incident or the final neutron energy to be one of only a few specific values. However, at a pulsed source the λ/n neutrons can be separated from the λ neutrons by their time of flight, eliminating the need for a filter. A TAS could therefore be operated more flexibly at a high flux spallation source allowing a wider choice of fixed incident or scattered neutron energies.

2.2 Indirect Geometry Crystal Analyzer Spectrometer

Figure (1b) shows a schematic diagram of an indirect geometry crystal analyzer time of flight spectrometer. The white pulsed neutron beam from the spallation source moderator is scattered by the sample. In practice it is not the full white beam which interacts with the sample since background choppers are used to remove unwanted high and low energy neutrons leaving an energy band which typically extends from 1 to 250 meV. Neutrons of a chosen final energy are Bragg reflected by an analyzer crystal into the detector where they are recorded as a function of their total flight time from the moderator to the detector. From this knowledge of the total time of flight and the final energy, the incident energy of the recorded neutrons and hence their wavevector and energy transfer to the sample can be calculated. The time of flight spectrum measured in the detector by such a spectrometer can therefore be transformed into a **spectrum along a path** in (**Q**, E) space as shown in figure (2) by the line A-B.

2.3 Direct Geometry Spectrometers

Figures (1c) and (1d) show two types of direct geometry time of flight spectrometer. The first employs a Fermi chopper to select a single neutron energy from the white pulsed neutron beam, while the second uses a monochromator crystal. The neutrons scattered from the sample at a single scattering angle into the detector are recorded as a function of their total time of flight from the moderator to the detector. In both cases the incident neutron energy is fixed by the monochromatisation process and the flight time of the neutrons from the moderator to the sample is therefore known. From a knowledge of the total and the moderator to sample flight times, the final neutron energy and hence the wavevector and energy transfer to the sample can be calculated. The time of flight spectrum recorded in the detector can be transformed into a **spectrum along a path** in (**Q**, E) space as shown in figure (2) by the line C-D.

2.4 The Constant-Q Scan

As shown in figure (2), for the same values of $\mathbf{k}_i$, $\mathbf{k}_f$ and ϕ, the direct and indirect geometry ToF instruments and the TAS all measure the counts at the same point (point O) in the constant-Q scan. For the ToF instruments these counts must, of course, be extracted by software from the time of flight spectra, but this is a trivial operation. The constant-Q scan is performed in the same way on all of these instruments, the $\mathbf{k}_i$, $\mathbf{k}_f$ and ϕ values are calculated for each point in the scan and the spectrometer measures each one in a step by step mode. The counting time required to measure a particular point in a constant-Q scan depends, apart from the scattering cross section of the sample, on the time integrated flux of the source, the transmission and reflectivity characteristics of the spectrometer components and on the desired resolution for the measurement. The overriding factor among these is the time integrated flux of the source. At an ESS type source, with a time integrated flux equal to that of the ILL high flux reactor, a constant-Q scan could be performed just as well by direct or indirect geometry ToF spectrometers as it could be by a TAS.

2.5 Multi-Analyzer and Multi-Detector Instruments

The considerations above were concerned with the performance of a constant-Q scan, or more generally, a single point step by step mode of taking data. However, while the TAS can **only** be operated in this mode, the ToF instruments have other modes of operation which are highly advantageous under the appropriate conditions. The single detector spectrometers shown schematically in figures (1b-d) will take a **whole spectrum** in the same counting time at an ESS type source that a TAS would take to collect one single data point. If the single detector is replaced by either a bank of detectors in the direct geometry case or a bank of analyzer-detector systems in the indirect geometry case (figures (3a-b)) then in the same counting time as a TAS measures a single data point, these spectrometers will measure a **surface** in (**Q**, E) space. Examples of these surfaces are shown in figures (4a) (multi-detector direct geometry spectrometer) and (4b) (multi-analyzer indirect geometry spectrometer). The data rate in these cases is of the order of 100 to 1000 times greater than that of the TAS.

The example presented in figure (4b) considered the case where all of the analyzer-detector units in the indirect geometry case were fixed at the same final energy E_f. However, this is not an exclusive requirement; the analyzing energies for the different analyzer-detector units can be different. Subject to (i) the mechanical constraint that

the detector arms cannot overlap and (ii) the condition that the E_f values should lead to a reasonable energy resolution, the analyzer energies can be chosen such that the (**Q,** E) surface forms a **vertical plane** [3]. The condition for this configuration is that $(\sin \phi_n / \sin \vartheta_{An})$ = constant for the n^{th} analyzer-detector unit, where ϕ_n is the scattering angle at the sample and ϑ_{An} is the Bragg angle of the analyzer. This situation is a unique mode of operation for indirect geometry multi-analyzer spectrometers and is illustrated in figure (4c). Such a mode is very attractive, if the (**Q,** E) plane can be conveniently arranged to be along a high symmetry direction.

In two-dimensional magnetically ordered crystals for example, the magnetic Bragg scattering takes the form of rods rather than points in reciprocal space and the excitation spectra depend only on the value of the wave vector perpendicular to the Bragg rod, $q_{\perp}$. The multi-analyzer system can be arranged such that the individual detectors scan parallel to the Bragg rod and thus measure the excitations for different values of $q_{\perp}$ simultaneously (see e.g. [4]). With chopper spectrometers a similar advantage can be taken when studying low dimensional systems. Here the symmetric arrangement of the detector banks is exploited to increase the count rate.

2.6 Rotating analyzer spectrometer

Another approach to exploiting the indirect geometry technique is being pioneered by the ROTAX instrument [5]. Here a single analyzer crystal undergoes a high speed non-linear rotation which is synchronized to the spallation source pulse. The neutrons are measured in a position sensitive detector as a function of their scattering angle from the analyzer crystal and their total flight time. In comparison with the multi-analyzer spectrometer discussed above, two relevant points should be made concerning the operation of a ROTAX-type instrument: a) measurements are made along a **single path** in (**Q**, E) space and b) this path can be directed along **any direction** in reciprocal space [6]. Although the data rate on such an instrument is lower than that of a multi-analyzer instrument, it has the advantage that longitudinal or transverse time of flight scans can be performed. Again, in comparison with a TAS at an ESS type source, a ROTAX type analyzer-detector system will take a whole spectrum in the same time that the TAS would require to measure a single data point.

2.7 A Flexible Spectrometer for Single Crystal Studies

The simplest way of categorizing a spectrometer for single crystal measurements is that it consists of 3 stages: a) an incident beamline stage, b) a sample orientation stage and c) a detector stage. All of the spectrometers described above can be categorized in this simple way. They all share the same type of sample stage, a goniometer device for

appropriately orienting the crystal and its sample environment in the beam. Another common feature in all cases is that the detector stage is rotated about the sample axis to vary the scattering angle(s) ϕ from the sample. The main difference between these instruments lies in the detector stages themselves: a single detector (fig. 1c), a single analyzer-detector (fig. 1b), a single rotating analyzer plus a multi-detector (ROTAX), a multi-detector system (fig. 3a) and a multi-analyzer-detector (fig. 3b) system. However, a suitable degree of standardisation means that all of these detector stages can be considered as **different detector modules** available on the **same instrument**.

This leaves the incident beamline stage. Although to the uninitiated it may seem a strange concept, the indirect geometry spectrometers (figure (1b)) and the Fermi chopper spectrometer of figure (1c) share the same incident beamline stage. It is a quick operation on the chopper spectrometers HET and MARI at ISIS to remove or replace the Fermi chopper in order to switch these instruments between mono-energetic or white beam modes. The white beam mode for example is used regularly during the alignment of single crystal samples on HET and MARI.

It is therefore easy to conceive of a highly flexible but simple ToF single crystal instrument which could exploit all of the possibilities available with the indirect and direct geometry modes of operation while maintaining the constant-Q capability. The incident beamline for such an instrument has an optional Fermi chopper allowing the choice between direct or indirect geometry modes. It has a standard goniometer to orient the crystal and its sample environment in the beam. There are then a number of optional detector stages, multi-analyzer, multi-detector, rotating analyzer etc., which can be mounted on an arm/table which rotates about the sample axis in order to vary the scattering angle ϕ for the detector(s). Such an instrument is not limited to inelastic measurements, but could also perform diffraction experiments using a multi-detector or area detector module.

The incident beam line designs of the TAS and of the direct geometry spectrometer shown in figure (1d) are however quite different. Because the monochromatisation process is carried out by Bragg reflection, it is necessary for the whole spectrometer to rotate about the axis of the monochromator crystal. Although this is a mechanical disadvantage, there are two reasons why it may be argued that it is desirable to employ a crystal monochromator. Firstly, a monochromator can be used to focus the neutron beam onto the sample point, something which cannot be done with a chopper or with the open beam used in indirect geometry. Focussing the incident beam in a measurement is of course done at the expense of the wavevector resolution. The

second reason is that a monochromator such as a Heusler alloy or an Fe(Si) crystal can be used to polarize a neutron beam. This is the only competitive argument for building a TAS instrument at a high flux spallation source, to perform studies which involve full polarization analysis using a polarizing monochromator and analyzer crystal. This argument would of course be changed by the advent of white beam polarizing filters [7].

3 Scientific Applications

In this section we discuss the additional scientific opportunities opened up by the characteristics of ToF spectrometers. Although it is clearly an oversimplification, it is, however, possible to classify different types of measurement carried out on single crystals by how much of (**Q**, E) space is sampled in the experiment. In the next 3 subsections the cases of large, intermediate and small regions of (**Q**, E) space are considered. Following this we discuss the possibilities for exploiting the time structure of a spallation source for pulsed sample environment and time resolved measurements. Finally the use of ToF spectrometers for some specialized diffraction measurements is briefly considered.

3.1 Large Regions of (Q, E) Space

In order to develop models of the atomic forces in crystalline solids, measurements of the phonon modes in many different Brillouin zones are required, i.e. many localized points in a large volume of (**Q**, E) space have to be sampled. Dorner discussed in ref. [1] phonon measurements on Al_2O_3 [8] where with a $4cm^3$ sample and with the high flux available on the TAS instruments at ILL it took 30 days of beam time to obtain this data along the high symmetry directions. However, it has long been recognized that the phonon dispersion relations along the high symmetry directions in a crystal do not by themselves provide a complete picture of the interatomic forces in a crystal and it has been advocated [9] that off-symmetry measurements are important as well. The collection of such a large amount of off-symmetry data would occupy a TAS instrument for a prohibitively long time and it was realized some time ago [10] that the parallel measuring techniques which can be employed with time of flight offered the possibility of performing such measurements in a reasonable amount of time.

The ToF surfaces described in section (2.4) (figures (4a) and (4b)) can be swept through the sections of the Brillouin zones that are intersected by the scattering plane, sampling all of the branches visible in these sections. Subject to the kinematic constraints on inelastic neutron scattering, any region in the scattering plane can be

sampled in this way with any choice of energy resolution by choosing the appropriate values of E_i or E_f. At an ESS type source a substantial fraction of the scattering plane could be mapped out by this method in the same time that it would take a TAS to complete a single constant-Q scan.

The problem which one faces when so much data is collected, so quickly, is how to analyze it. This is, however, not a question of physics but a question of software development, ie. the construction of algorithms which extract from the measured spectra the phonon dispersion surfaces which gave rise to those spectra. As yet no such software exists: time and manpower will have to be committed to write such code. However, even when such software is available it is probable that the "surface" scans described above would not be the only input data to such analysis programs. The inclusion of constant-Q scans at specific high symmetry wavevectors, of ROTAX type time of flight scans along fundamental symmetry directions and of "vertical plane" scans (figure (3c)) along high symmtery directions would all help to provide "boundary conditions" in the analysis. The vertical plane scans are an attractive option, combining the data rate of a surface scan with a high symmetry direction. As an illustrative example we show in figure (5) the magnetic excitation spectrum in $TbFeO_3$ [11] measured along two different crystallographic directions. The dispersive spin wave modes and the crystal field levels are clearly visible. However, this mode of operation is restricted to a certain extent by mechanical and resolution criteria. The extent of these limitations is discussed in more detail in the appendix.

3.2 Intermediate Regions in (Q, E) Space

The measurement of complete sets of phonon dispersion relations is only one small part of the interest in studying excitations in single crystals. Although the volume sampled in such measurements is large, the phonons themselves are usually well defined sharp excitations. There is also, however, a great interest in studying systems where the excitations, phonon or spin wave modes, are broad, sometimes even to the extent that the concept of a dispersion curve does not really apply anymore and the inelastic response is best presented as an intensity map of $S(\mathbf{Q}, E)$ over a region of ($\mathbf{Q}$, E) space. Such a region would generally be of the same order as the size of the Brillouin zone. Clearly, measurements of features extending over such a range can be done very efficiently with ToF techniques.

As an example we present here experiments carried out on calcite (rhombohedral crystal structure) by Dove et al. [12] using the PRISMA spectrometer. Initial measurements using a TAS had indicated that the dispersion relation of the Γ-F

transverse acoustic (TA) phonon branch in calcite dips down in energy at the F-point. In order to obtain a global picture of the scattering the "vertical plane" configuration was used (see figure (4c)), with the plane oriented along the Γ-F direction from the (3.5,0,2) to the (2.5,0,-2) F-points. Three adjoining "vertical plane" settings covered the whole range of interest and were used to map out S(**Q**,E). The results were reported in [12] in a conventional presentation, i.e. with spectra (counts as a function of energy transfer) and 1-dimensional dispersion relations. In figure (6) we show an alternative way of presenting the data as a "3-D topographic" visualization. It should be emphasized that the raw data has been used to create this surface, not a theoretical model. The large peak in the background of the plot is the (3,0,0) Bragg peak with the low energy acoustic phonons emerging from it, while in the foreground the TA phonons at the F-point (2.5,0,-2) in both energy gain and loss appear as large "mountain" features. The intensity of these modes can be contrasted with the much lower intensity of the TA branch joining the (3,0,0) to the F-point. Between the energy loss and gain TA modes at the F-point, there is a bridge of inelastic scattering. It is easy to extract, from the data set shown in figure (6), "conventional" scans and in figures (7a-b) respectively, we show a constant-Q extraction at the F-point and a series of constant-E extractions at different energy transfers through the F-point.

This bridge of scattering had not been recognized in the initial TAS experiment, but once its existence was realized it was subsequently observed using a TAS as well [12]. It had been missed in the first TAS measurements for a combination of two reasons. Although the column is quite clear in a constant-E scan, it is not as clear in the constant-Q scan at the F-point. This problem is exaggerated because the F-point is at a position where the λ/2 contamination is a particularly bad problem for a TAS operating with a steady state beam. Only when the overall behaviour over a region of (**Q**, E) space around the F-point is visualized does the full picture become readily apparent.

Another example of where an extended region of (**Q**, E) space around a particular wavevector has to be investigated, is dynamical critical scattering. Here the energy fluctuations are relatively small but depend upon the wavevector and are spread over a region of wavevectors around an ordering wavevector. In order to define S(**Q**, E) at a particular temperature a series of inelastic spectra must be taken at a sufficiently large number of wavevectors around the ordering wavevector. This must then be repeated at a large enough number of temperatures, so that an accurate temperature dependence can be obtained for the parameters derived from fitting the inelastic spectra. The ToF technique can do this rapidly by measuring slices through S(**Q**,E) (cf. figures (4a,b,c))

in parallel and by stepping the sample to measure perpendicular to the scattering plane. Such measurements can easily be combined with white beam diffraction measurements on the same instrument, carried out with higher neutron energies, to measure the isothermal susceptibility over the wavevector region of interest.

3.3 Small Regions in (Q, E) Space

The example of calcite in the previous subsection was chosen for a good reason. Once the existence of the column of scattering at the F-point had been identified, the scientific interest focused onto the small region of (**Q**,E) space at the F-point itself. The ToF techniques have advantages in data rate when they can be exploited to measure many data points in parallel. If, however, the measurements are concentrated into a small region in (**Q**,E) space, then the step-by step constant-Q mode of operation is most appropriate. At present, this type of measurement is best done with a TAS at a reactor source. With an ESS type source which will combine the advantages of present day high flux reactors and spallation sources, it will be easy to switch from a survey-type ToF experiment to a constant-Q mode measurement, without having to change to another instrument. At most this would involve changing a detector module, although in many cases it would amount to no more than a software operation to switch from using all of the analyzer-detector units to using just one.

3.4 Exploiting the Time Structure of a Spallation Source

In the previous sections we discussed how ToF techniques can be exploited to carry out "conventional" single crystal inelastic experiments. However, there are other opportunities for single crystal experiments which arise because of the pulsed time structure of the beam from a spallation source.

One such area is the exploitation of white beam techniques for real time measurements in single crystals. Studying the kinetics of the structural and dynamical changes of a system in connection with e.g. a phase transition or a chemical reaction, would provide a wealth of unique information.

An example of such real time behaviour is the growth of the superlattice at the order-disorder transition in alloys such as Cu_3Au and Ni_3Mn. At high temperature the two components are randomly disordered, but on quenching through the transition temperature they order onto particular sites in the lattice. This process can take from a few minutes to many hours, depending on quench temperatures and rates. Studying the non-equilibrium phonons in such a system cannot of course be done with the step by step technique of a TAS, since each step in the scan would be taken at a different real

time. However, with the ToF techniques discussed in section (2) a surface covering the region of interest in (**Q**,E) space can be chosen and since the spectra which make up the surface are collected in parallel, S(**Q**,E) can be collected in "slices" of real time. If one recalls that the corresponding measuring time at an ESS type source would be the same as for a TAS to measure a single data point, then the possibilities become strikingly clear.

The type of measurement described above is in fact already possible at present day spallation sources. Because the spectrometer does not move during the data taking period, the size of the real time slices in which the data is taken can be extremely short and subsequently added together by software to achieve the necessary statistical accuracy. Under these circumstances real time itself becomes a parameter in such an experiment and can be varied by software. The increased flux of an ESS type source when compared to ISIS will reduce the number of real time slices which are required for the necessary statistics and hence greatly improve the real time resolution.

As far as faster real time processes are concerned, we have developed at ISIS a technique which allows us to measure time-dependent phenomena on the millisecond scale. This technique applies to processes which are reversible and which can be induced by an external parameter which is triggered by the electronic signal generated when the spallation source neutron pulse is produced. A feature in the time of flight spectrum, e.g. a Bragg peak or a phonon, which is measured at a time t_1 is therefore measured at a real time $t_1 - t_f$ (where t_f is the sample to detector flight time) after the application of the external trigger. If a delay time t_0 is introduced into the circuit between the spallation source and the external trigger then the real time for the measurement is $t_1 - t_f - t_0$ and this can be "scanned" in a step by step mode by varying the value of t_0. If the timescale of the phenomenon is longer than one frame of the spallation source then it is also possible to "daisy-chain" together n of the time frames and to use only one out of every n spallation source pulses to trigger the external parameter. This technique has been used on PRISMA to examine the real time dependence of the incommensurate to ferroelectric transition in Rb_2ZnCl_4 when driven by an external electric field [13].

So far this millisecond time-resolved work on PRISMA has only involved Bragg diffraction experiments. However, in the near future we expect to extended this technique to both diffuse and inelastic scattering measurements. The high flux of an ESS type source will make such studies relatively straightforward.

Another situation where it will be possible to exploit the white beam techniques available with a spallation source are experiments with a sample environment which is phased to the production of the neutron pulse. An example of this is the use of pulsed high magnetic fields. This technique is being developed at the KENS spallation source in Japan [14] and although it has been applied so far only to diffraction studies, the advantages discussed above for performing inelastic scattering measurements apply equally well to this case.

3.5 Diffraction Measurements

At reactor sources there are some specialized single crystal diffraction measurements that are carried out using a TAS rather than a four circle diffractometer. These are measurements of critical or diffuse scattering. The reason for using a TAS is the need for good Q-resolution, which is provided by the Soller collimation. The same argument applies at a spallation source. Additionally, the white beam diffraction technique combined with a multi-detector means that regions of diffuse or critical scattering can be measured in parallel. At ISIS this technique has been used on PRISMA for a number of studies: the magnetic critical scattering from $FeCO_3$ [15] and terbium [16] and the ferroelastic transition in Na_2CO_3 [17]. In figure (8) we present results from the critical scattering in terbium. Such measurements would be well carried out by a flexible spectrometer of the type described in section (2.5).

4 The PRISMA Spectrometer

In the foregoing sections we have discussed the possibilities with time of flight techniques at *future* high flux spallation sources but only touched upon the situation at *present*-day sources. At ISIS inelastic single crystal measurements are performed on PRISMA (multi-analyzer spectrometer), ROTAX (rotating analyzer spectrometer) and the two chopper instruments, HET and MARI. The experience gained on MARI and HET has led to funding for the MAPS project [18], a dedicated chopper spectrometer for single crystal studies. The new features of MAPS, position sensitive detectors covering a large solid angle and a secondary flight path of 6m, will offer a substantial improvement in both count rate and resolution over HET and MARI. The ROTAX spectrometer is coming to the end of its commissioning phase and the results will be reviewed elsewhere. At the KEK/KENS spallation source inelastic single crystal measurements are carried out on the MAX spectrometer [19]. MAX was installed in 1980 and, like PRISMA, is a multi-analyzer instrument using 15 pyrolitic graphite analyzers. The development programme on MAX has been reported elsewhere [20] and has included the "low-dimensional" measuring configuration described in section (2.5) and the use of focussed analyzer crystals in a multi-analyzer system. In the

following we will outline the evolution of the PRISMA spectrometer and its future development.

PRISMA is a collaborative project between the Italian CNR, through the ISM at Frascati and the UK EPSRC, through the Rutherford Appleton Laboratory. This collaboration arose from earlier joint work on the CQS spectrometer at the HELIOS pulsed source at Harwell Laboratory [21]. The spectrometer was designed and constructed by the ISM [22] and installed at ISIS in 1987. Commissioning and initial measurements were carried out in 1988/89 [3]. Since then there has been a continual development programme which has included changes to the shielding, collimation and analyzer crystals and the inclusion of a background chopper in the incident beamline [23]. During the same period the ISIS source itself has also undergone change with the proton current increasing by a factor of 10. The development work on PRISMA has been aimed not only at improving the performance of the present instrument but also at identifying new techniques such as the real time and critical scattering studies referred to earlier and how the overall spectrometer configuration itself could be optimized to take account of new opportunities.

This last aspect has demonstrated to us the need for the instrument design to contain a high degree of flexibility and during the last year work has progressed on modifications to the PRISMA spectrometer to achieve this. The underlying criteria in this work has been that the instrument should not lose its present capabilities, but rather that new possibilities should be opened up and that it should be easy to integrate further options in the future, if and when they arise. In this respect PRISMA is evolving towards the flexible spectrometer described in section (2.5). At this time it is not intended that PRISMA should have a Fermi chopper or a ROTAX module, but rather that it should allow a wide selection of indirect geometry options to be used. Initially three detector modules will be available, (a) the current PRISMA multi-analyzer system for survey measurements, covering a wide range in (Q,E), (b) a multi-double-analyzer system (see ref.[24]) and a multi-detector diffraction system for critical and diffuse scattering studies. In the future there are plans to include both a further multi-analyzer system with a wider angular separation between the analyzers and a polarization analysis system.

5 Summary

In this paper we have compared the operational characteristics of a triple axis spectrometer at a next generation high flux spallation source [2] with those of time of

flight spectrometers. We have argued that at such a source the constant-Q type scan will be equally well performed by time of flight spectrometers as by a TAS at present day reactor sources or indeed on the ESS. However, the time of flight character of the measurements at a spallation source means that for many experiments a very much higher data rate can be obtained using direct and indirect geometry spectrometers. In particular the indirect geometry spectrometers offer a high degree of flexibility and can perform new types of measurement which would be difficult or impossible to do with a TAS. The potential of some of these new techniques has already been demonstrated at present day spallation sources.

The PRISMA spectrometer at ISIS is currently undergoing modifications which will increase its capabilities for single crystal neutron scattering experiments. The principal feature of the modifications is that the instrument can be used with different detector modules which can be easily interchanged. Initially three modules will be available, the current multi-analyzer-detector system, a new double-analyzer-detector system and a diffraction detector for critical and diffuse scattering studies. The standardization of mounts and cabling for these units means that in future other modules can be envisaged, e.g. a widely spaced multi-analyzer-detector system or a polarization analysis system.

Exploring the full potential of time of flight techniques for single crystal studies requires both further technical development and also the development of new computer software to visualize, model and fit the data taken. The computer hardware for doing the latter is available today, what is missing is the manpower to construct the algorithms needed to tackle these tasks. A source like the ESS will offer many new and unique possibilities for single crystal neutron scattering. Exploiting these opportunities is a challenge!

Acknowledgement

We would like to thank C J Carlile, M T Dove and M J Harris for helpful discussions. The financial support of the Italian Consiglio Nazionale delle Ricerche for the PRISMA development project is gratefully acknowledged.

Appendix

In figures (4a-c) three measuring surfaces for different time of flight geometries are shown. The third geometry, the "vertical plane", is unique to the multi-analyzer spectrometers, such as PRISMA and MAX, because it requires each analyzer-detector unit to have a different value of E_f. The attraction of this geometry is that the vertical plane can be arranged along a desired direction in a crystal. In this case the data collection rate is very high. For example the results for calcite shown in figure (6) were collected on PRISMA some time ago now. Taking into account the intervening developments on PRISMA and the increase in ISIS current since then, this data could be collected now in 1 hour. At an ESS source, which would be ~30 times brighter than ISIS, this would correspond to 2 minutes! This applies of course to the measurements of low energy excitations, up to ~15meV, while in his experiment on Cr_2O_3 Dorner [1] measured phonon branches up to and including 80meV. If the data on Cr_2O_3 presented in figures (6) and (7) of ref. [1] were to be taken at an ESS type source using a multi-analyzer spectrometer it could be collected in less than 20 minutes. The full exploitation of such data rates will depend upon particular experiments, perhaps to carry out real time studies or a careful temperature dependence or to survey an area in (Q,ω) space to look for a particular feature before studying them in more detail with a "constant-Q" type measurement.

The attraction of the vertical plane geometry must however be tempered with a knowledge of its limitations. The restrictions on its use arise from three criteria (i) the available range of scattering angles ϕ on an instrument, (ii) that the analyzing energies should not lead to unreasonable resolution criteria and (iii) that the detector arms cannot physically overlap. Before considering these points in further detail there is an important point that should be made. For any particular vertical plane (determined by a wavevector in the plane, the direction of the plane and an energy transfer in the plane) there is only one set of analyzing energies which correspond to this plane [3].

The first two criteria lead to an "available measuring area" in reciprocal space for a particular energy transfer. In figure (9) we show the available area in the wavevector co-ordinates $Q_{\parallel}$ and $Q_{\perp}$ for a multi-analyzer spectrometer for zero energy transfer with $E_{f,min}$ = 18meV, $E_{f,max}$ = 45meV and a maximum scattering angle ϕ of 125° (solid line). The wavevectors $Q_{\parallel}$ and $Q_{\perp}$ are measured from the origin of reciprocal space and are parallel and perpendicular to the vertical plane respectively. The boundaries of this area are governed in the following way. The section A-B arises from the minimum

value of E_f , the section B-C from the maximum ϕ angle and the section C-A from the maximum value of E_f. The dashed line in figure (9) corresponds to the measuring area at zero energy transfer for a multi-analyzer system with a minimum E_f of 6meV, a maximum ϕ of 160° and a maximum E_f of 45meV.

The final criteria (iii), depends upon the exact parameters of the multi-analyzer-detector arm. This can be seen by noting that in the hypothetical case of an infinite sample to analyzer distance L_{SA}, there would never be any overlap of the detectors. In practice of course L_{SA} must be a reasonable (non-infinite) distance. The current multi-analyzer system on PRISMA has 16 analyzer-detector units, each separated by 2^{o} in scattering angle with $L_{SA} = 0.58$m and an analyzer to detector distance of 0.17m. The minimum analyzing energy is 18meV (for pyrolitic graphite analyzer crystals) and the maximum ϕ angle is 125°, corresponding to the area marked by the solid line in figure (9). Within this particular region there are no overlap limitations for pyrolitic graphite analyzers. An expansion to the region bounded by the dashed lines requires modifications. The increase in the maximum ϕ angle to 160° will occur through the current modifications to the PRISMA beamline. The reduction in the minimum value of E_f to 6meV would, however, require modification to the multi-analyzer arm itself, either by increasing the angular separation from 2^{o} to 4^{o} or by changing L_{SA} to 1.0m. If all other parameters remained the same then either of these changes would allow the dashed area in figure (9) to be free of overlap restrictions.

If one wished to use values of E_f less than 6meV then it is essentially impossible with a bank of single pyrolitic graphite analyzer crystals. Although it is possible to use a bank of analyzer crystals with a much larger d-spacing, such as mica for example, their reflectivity is much lower. However, another way to achieve lower analyzing energy is to use a double-analyzer crystal device. Such a multi-double-analyzer system which will allow analyzer energies down to 2.25meV has been designed and is under construction in Italy with the financial support of the CNR. A report on the evaluation of a double-analyzer prototype is given by Petrillo et al in [24].

References

[1] B. Dorner, J. of Neutron Research **2/3**, 115 (1994)

[2] Instrumentation & Techniques for the European Spallation Source, Report of an Expert Meeting held in Abingdon, 1992, Editor A.D.Taylor; also H.Lengeler and J.L.Finney, *The European Spallation Source*, Europhysics News, **25**, 37 (1994)

[3] U. Steigenberger , M.Hagen, R Caciuffo, C.Petrillo, F.Cilloco and F.Sacchetti, Nucl. Inst. and Meth. **B53**, 87 (1991)

[4] Y.Todate, H.Ikeda, K.Shibata, K.Tajima and Y.Endoh, J.Phys.Condens.Matter **1**, 5895, (1989)

[5] H.Tietze-Jaensch, W.Schmidt, D.Sieger, R.Geick and U.Steigenberger, Physica **B180&181**, 920 (1992) and references therein

[6] W Schmidt, H.Tietze-Jaensch and R.Geick, Proceedings ICANS-XII, Rutherford Appleton Laboratory Report **94-025**, I-292 (1994)

[7] Y.Masuda, K. Asahi, M.Doi, K.Sakai, H.Sato and Z.Z.Jian, Proceedings ICANS-XII, Rutherford Appleton Laboratory Report **94-025**, I-338 (1994) and F.Tasset, T.E.Chupp, J.P.Pique, A.Steinhof, A.Thompson, E.Wassermann and M.Ziade, Physica **B180&181**, 896 (1992)

[8] H.Schober, D.Strauch and B.Dorner, Z.f.Physik **B92**, 273 (1993)

[9] D. Strauch, Arbeitstreffen des Verbundes Forschung mit Neutronen, Berlin 1990

[10] G. L. Squires, Proc. Phys. Soc. **88**, 919 (1966) and R.Pynn and G.L.Squires, Proc. R. Soc. Lond. **A326**, 347 (1972).

[11] A.Goukasov, Experimental Report, ISIS'93 288 (1993)

[12] M. T. Dove, M.Hagen, M.J.Harris, B.M.Powell, U.Steigenberger and B.Winkler, J. Phys. Cond. Matter **4** 2761 (1992)

[13] U.Steigenberger, G.Eckold and M.Hagen, Nucl. Inst. and Meth. **B93**, 316 (1994)

[14] H.Nojiri, M.Motokawa, N.Nishida and Y.Endoh, Physica **B180&181**, 31 (1992) and M/Motokawa, M.Arai, M.Mino, K.Ubukata, T.Bokui and M.Fujita, Proceedings ICANS-XII, Rutherford Appleton Laboratory Report **94-025**, I-260 (1994)

[15] S.J.Payne, M.J.Harris and M.Hagen, to be published

[16] M.Hagen, R.S.Eccleston, S.J.Payne and S.B.Palmer, to be published

[17] M.J.Harris and M.T.Dove, to be published

[18] T.G.Perring, A.D.Taylor, R.Osborn, D.M.Paul, A.T Boothroyd and G.Aeppli, Proceedings ICANS-XII, Rutherford Appleton Laboratory Report **94-025**, I-60 (1994)

[19] K.Tajima, Y.Ishikawa, K.Kanai, C.G.Windsor and S.Tomiyoshi, Nucl. Inst. and Meth. **201**, 491 (1982)

[20] Y.Todate, H.Ikeda, K.Tajima and S.Tomiyoshi, Proceedings ICANS-XI, KEK Report **90-25**, 739 (1990)

[21] C.Andreani, P.Bosi, E.Mazzega, F. Sacchetti and C.G.Windsor, J.Phys.C16, 3055 (1983)

[22] C.Andreani, C.J.Carlile, F.Cilloco, C.Petrillo, F.Sacchetti, G.C.Stirling and C.G.Windsor, Nucl. Inst. and Meth. **A254**, 333 (1987)

[23] U.Steigenberger, M.Hagen, C.Petrillo and F.Sacchetti, Proceedings ICANS-XI, KEK Report **90-25**, 743 (1990)

[24] C. Petrillo, F.Sacchetti, M.Hagen and U.Steigenberger, RAL Report RAL-93-091

Figure captions

Figure 1

Schematic diagrams of (a) a triple axis spectrometer (TAS), (b) a Fermi chopper based direct geometry spectrometer, (c) a crystal analyzer indirect geometry spectrometer and (d) a monochromator based direct geometry spectrometer, are shown.

Figure 2

A constant-Q scan (crosses) is shown in relation to the measuring paths taken by indirect geometry (A-B) and direct geometry (C-D) time of flight spectrometers.

Figure 3

Schematic diagrams are shown of (a) a multi-analyzer spectrometer and (b) a multi-detector spectrometer.

Figure 4

(a) The measuring surface of a direct geometry time of flight spectrometer is shown.
(b) The measuring surface of an indirect geometry time of flight spectrometer with all analyzers set to the same final energy is shown.
(c) The measuring surface of an indirect geometry time of flight spectrometer with the analyzer energies set according to the relation $(\sin \phi_n / \sin \vartheta_{An}) = \text{constant}$.

Figure 5

The spin wave and crystal field modes in $TbFeO_3$ measured on PRISMA using the "vertical plane" geometry.

Figure 6

A 3-D topographic visualization of the soft TA phonons and the column of scattering at the F-point in calcite.

Figure 7

Conventional representations of the data shown in figure 6 which have been extracted as (a) a constant-Q scan at the F-point and (b) constant-E scans through the F-point along the Γ-F direction at energy transfers of 0, 1, 2, and 3 meV.

Figure 8

The data collected in a diffraction measurement of the critical scattering from Terbium slightly above the Neél temperature is shown as a contour map.

Figure 9

The available area in the wavevector co-ordinates $Q_{||}$ and $Q_{\perp}$ for a multi-analyzer spectrometer for zero energy transfer with $E_{f,min}$ = 18meV, $E_{f,max}$ = 45meV and a maximum scattering angle ϕ of 125° (solid line). The dashed line corresponds to the measuring area at zero energy transfer for a multi-analyzer system with a minimum E_f of 6meV, a maximum ϕ of 160° and a maximum E_f of 45meV.

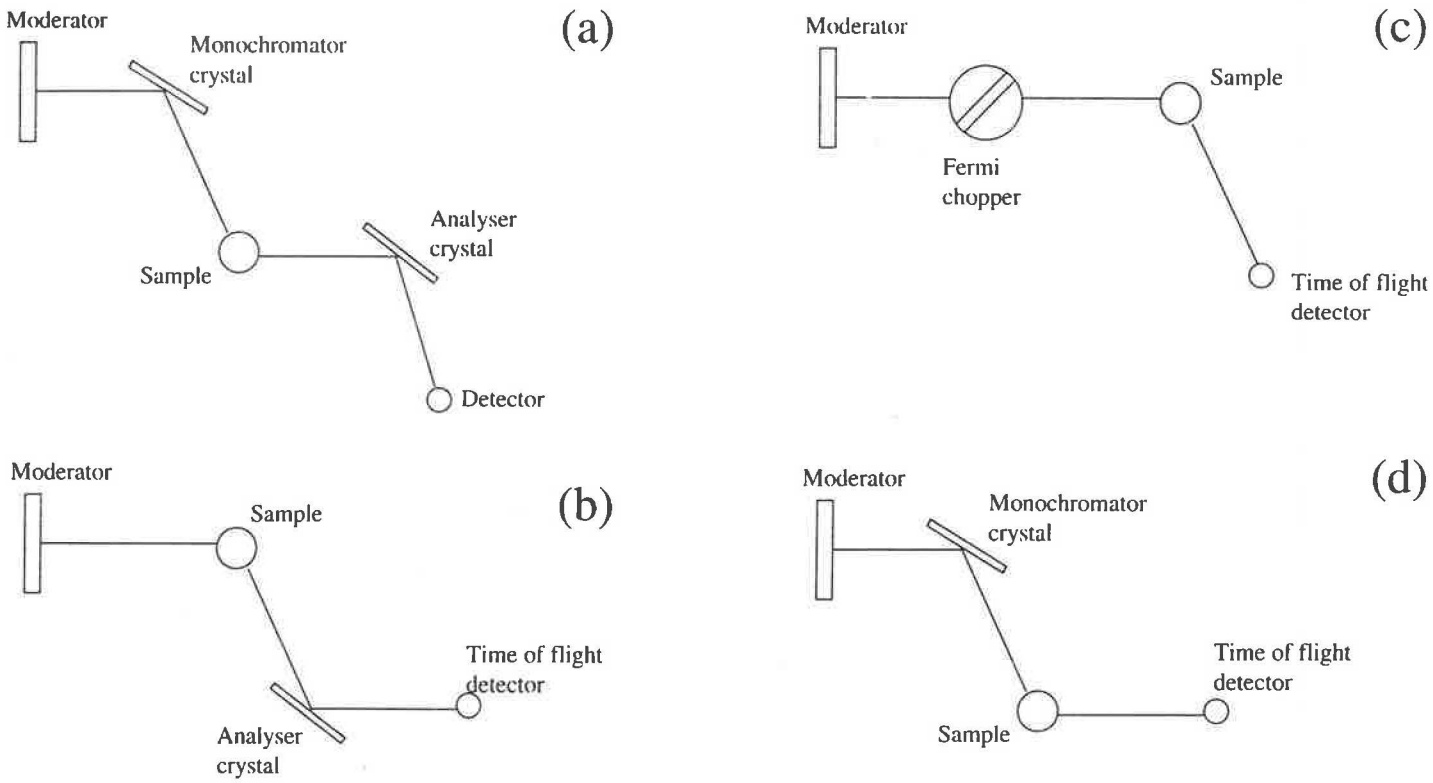
(a)
Moderator
Monochromator crystal
Analyser crystal
Sample
Detector
(b)
Moderator
Sample
Time of flight detector
Analyser crystal
(c)
Moderator
Sample
Fermi chopper
Time of flight detector
(d)
Moderator
Monochromator crystal
Time of flight detector
Sample

Fig. 1

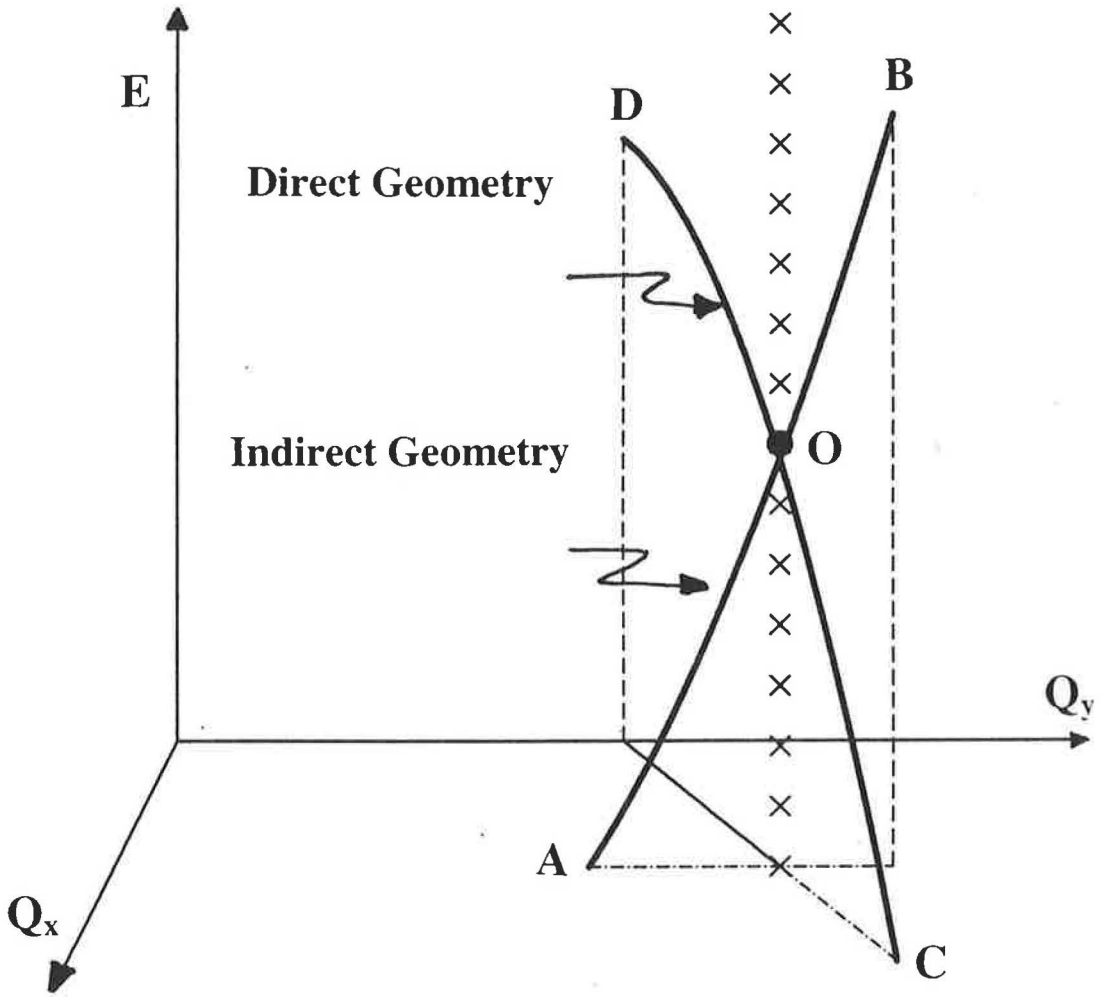

Fig. 2

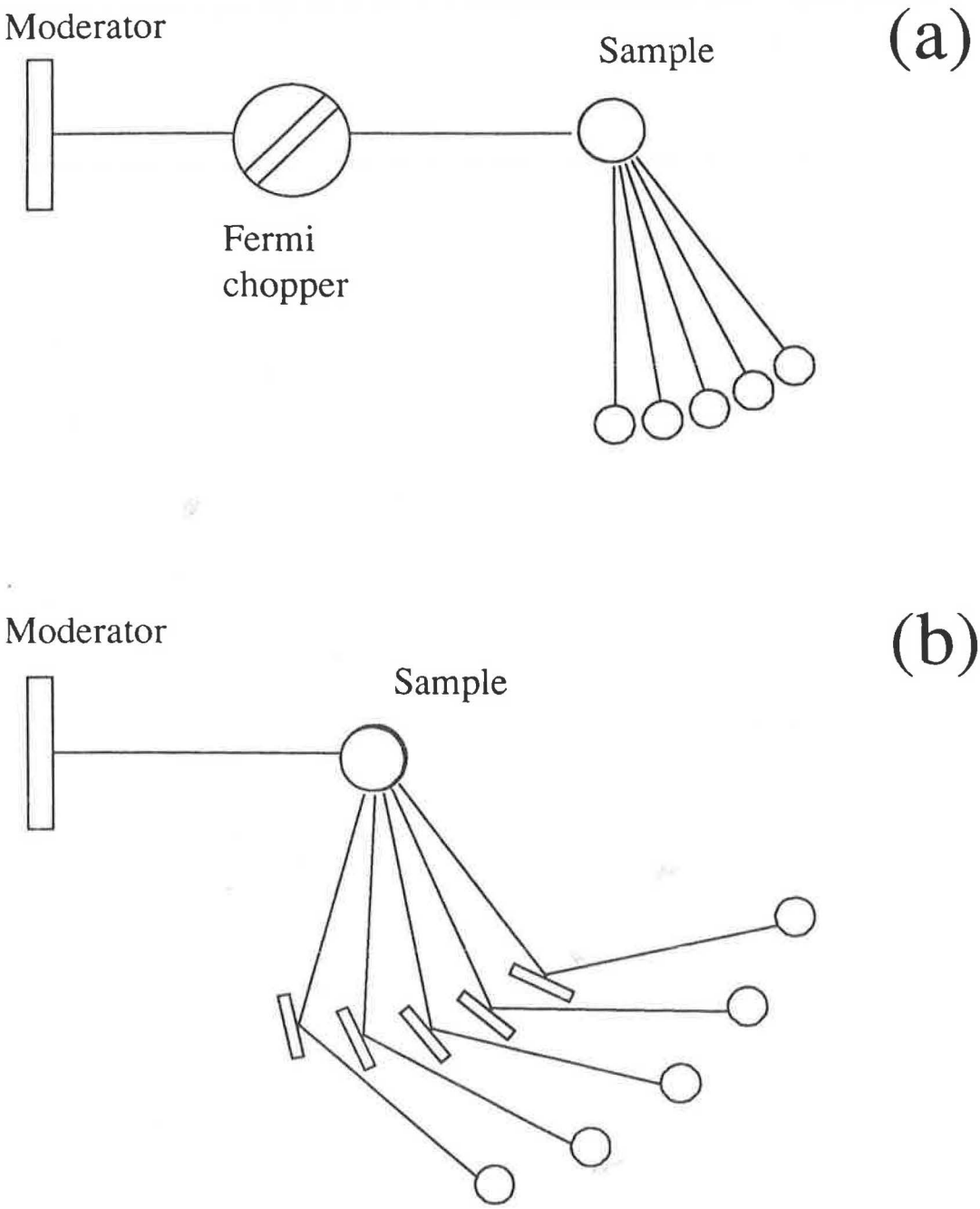

Fig. 3

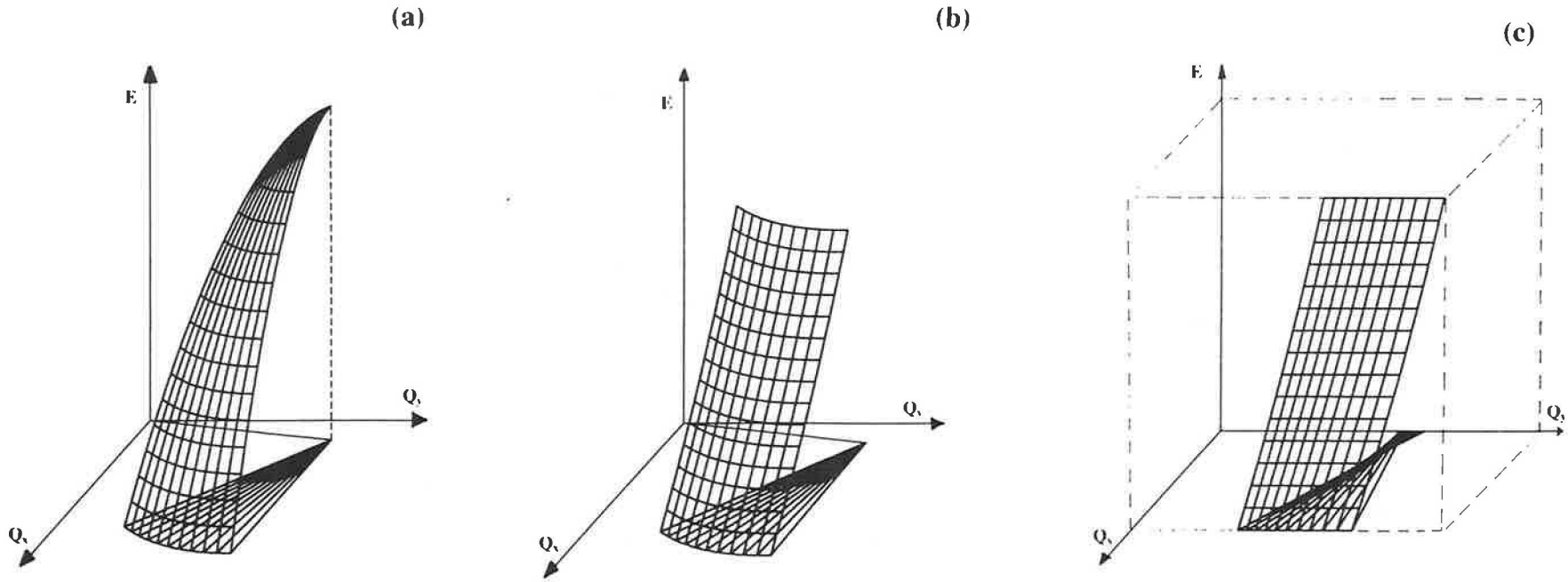

Fig. 4

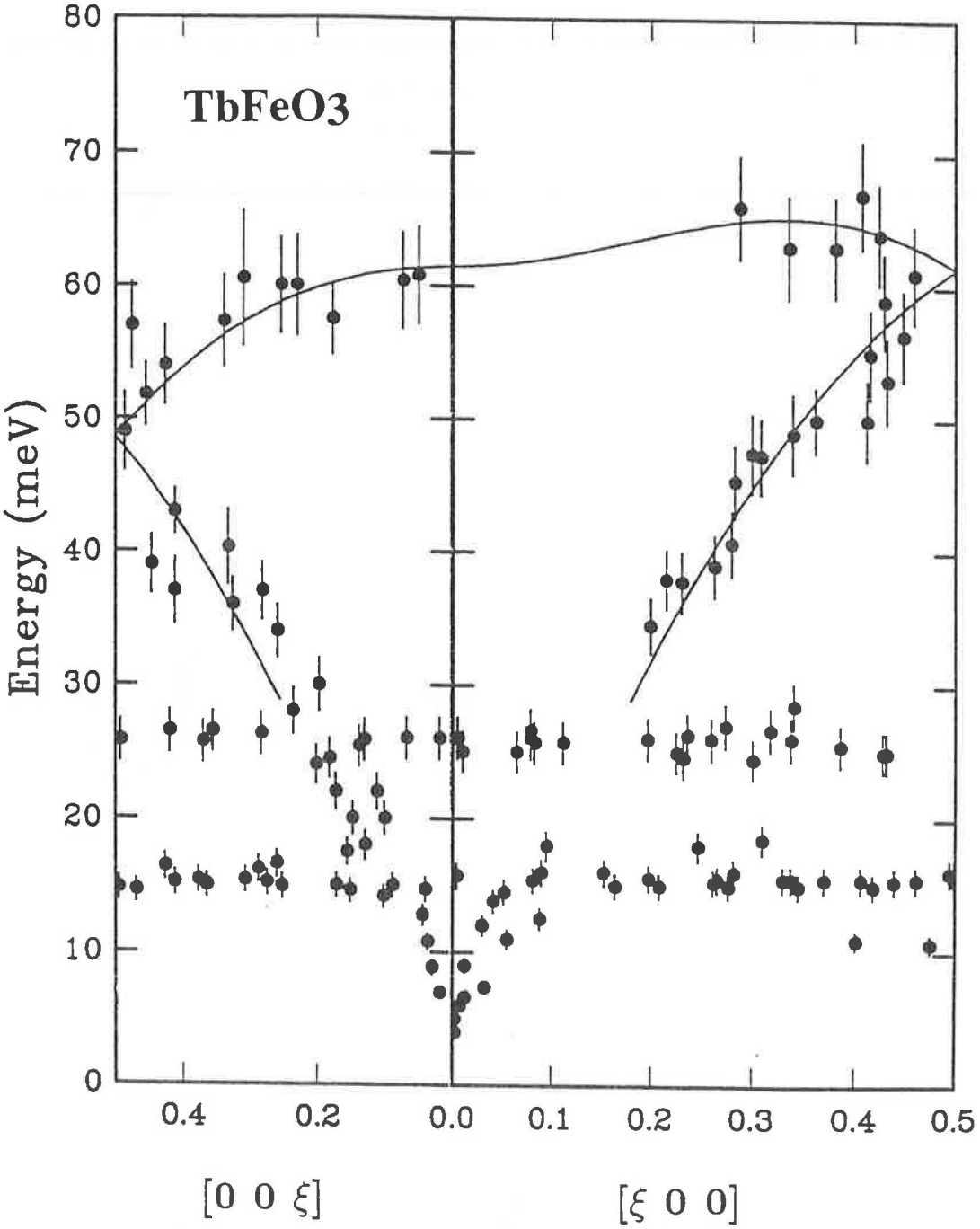
TbFeO3
Energy (meV)
80
70
60
50
40
30
20
10
0
0.4
0.2
0.0
0.1
0.2
0.3
0.4
0.5
[0 0 ξ]
[ξ 0 0]

Fig. 5

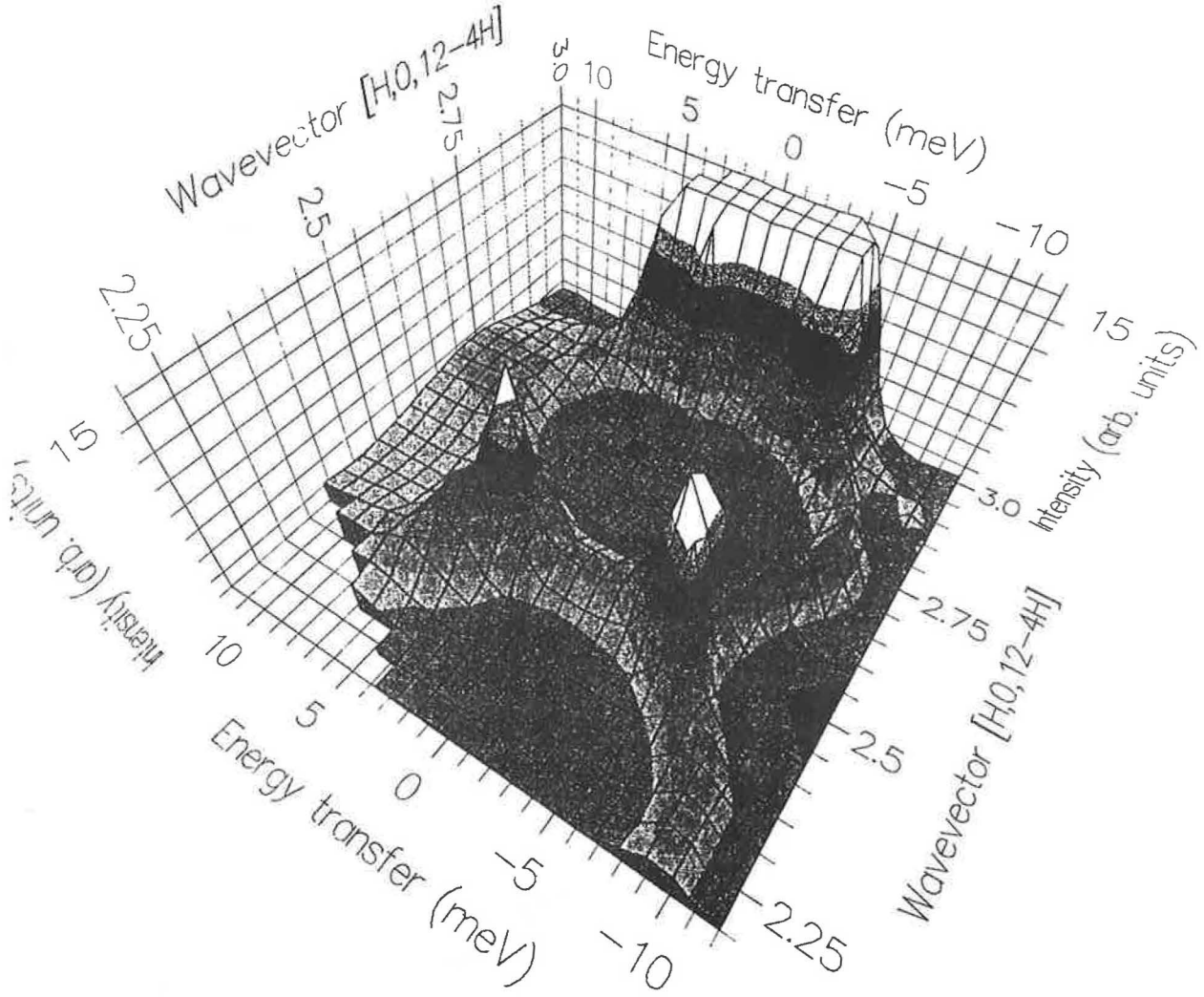
Wavevector [H,0,12-4H]
2.5
2.75
3.0
Energy transfer (meV)
10
5
0
-5
-10
15
Intensity (arb. units)
2.25
2.5
2.75
3.0
Wavevector [H,0,12-4H]
2.25
Energy transfer (meV)
10
5
0
-5
-10
15
Intensity (arb. units)

Fig. 6

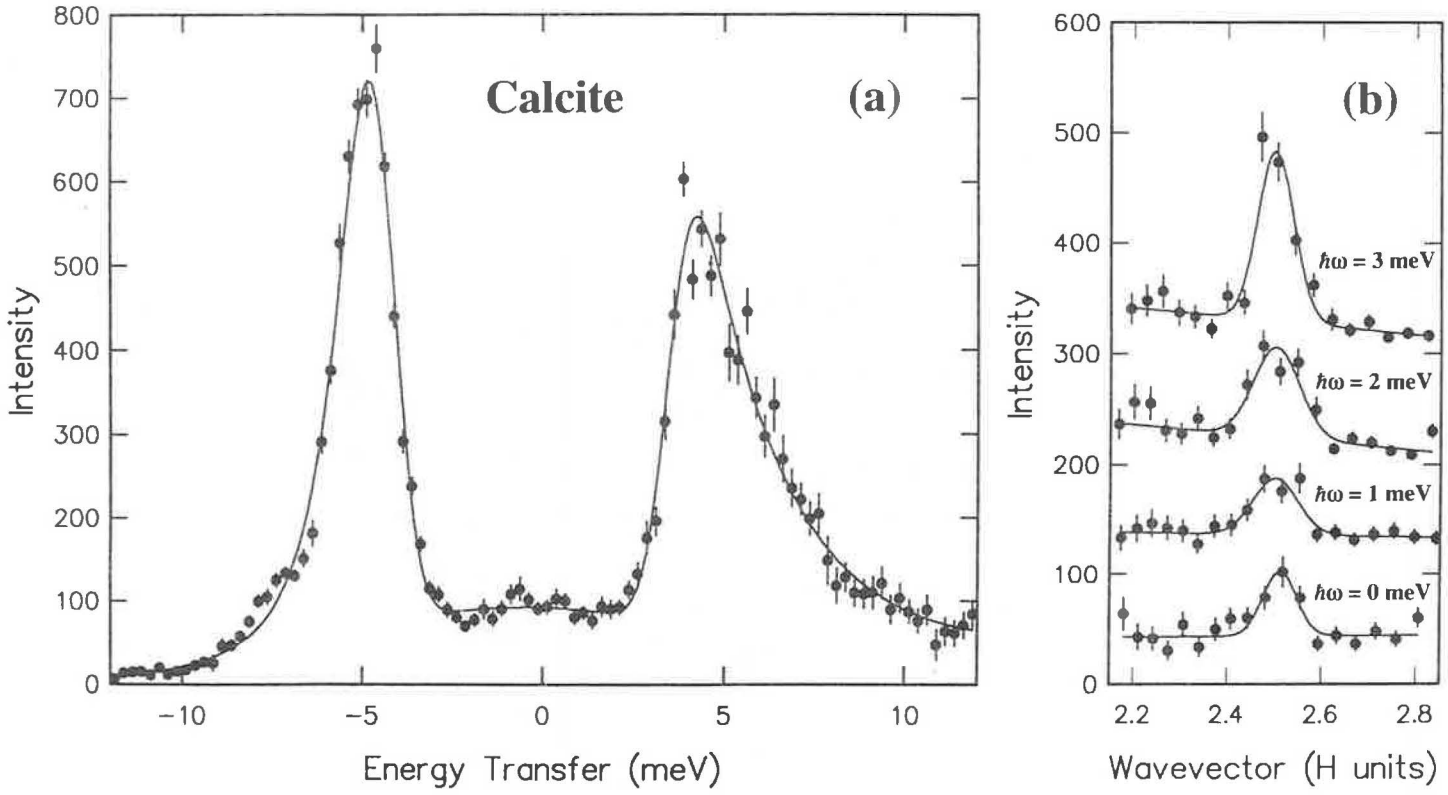
Calcite
(a)
(b)
Intensity
Energy Transfer (meV)
Wavevector (H units)
ħω = 3 meV
ħω = 2 meV
ħω = 1 meV
ħω = 0 meV

Fig. 7

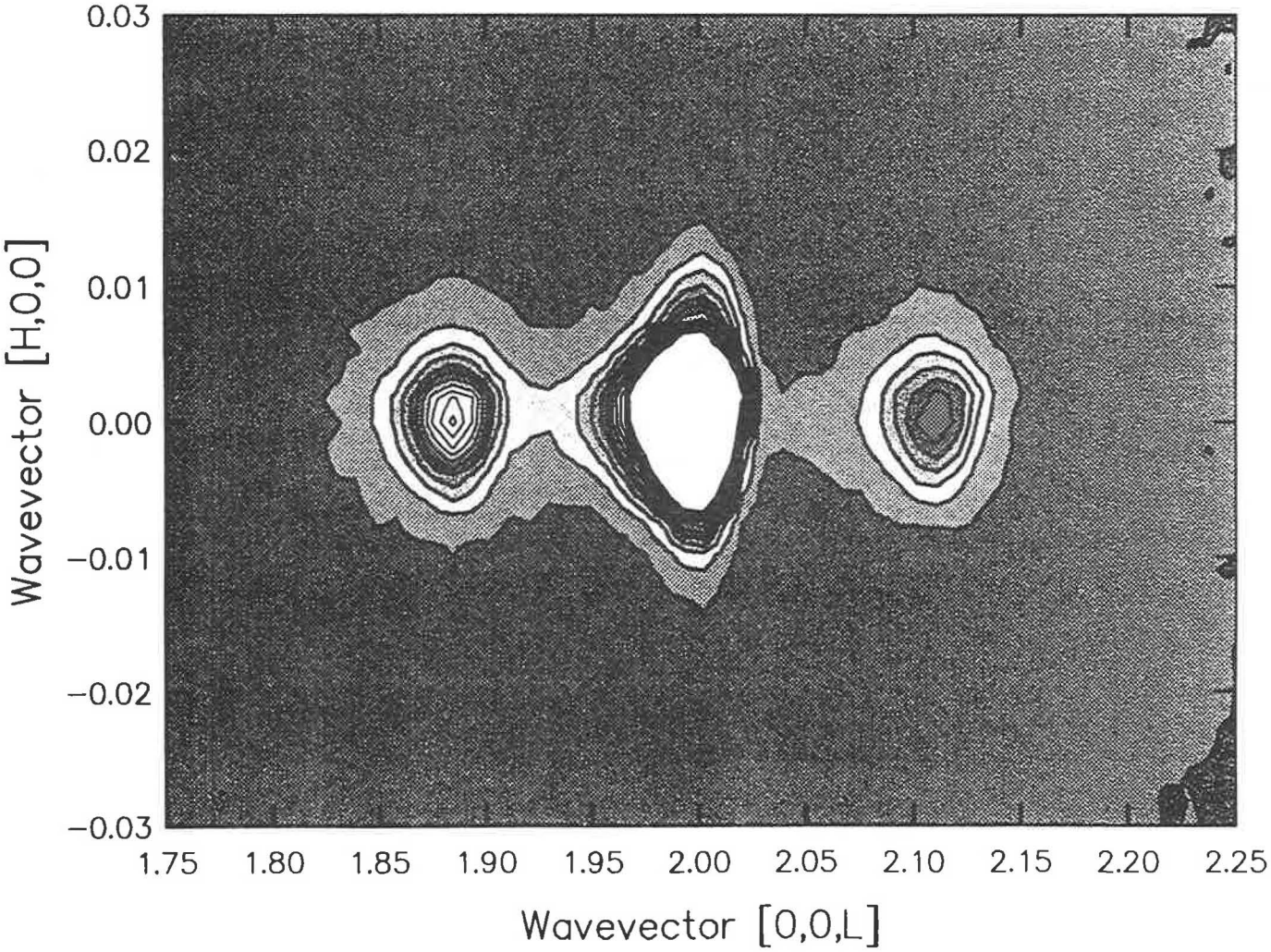
0.03
0.02
0.01
0.00
−0.01
−0.02
−0.03
Wavevector [H,0,0]
1.75
1.80
1.85
1.90
1.95
2.00
2.05
2.10
2.15
2.20
2.25
Wavevector [0,0,L]

Fig. 8

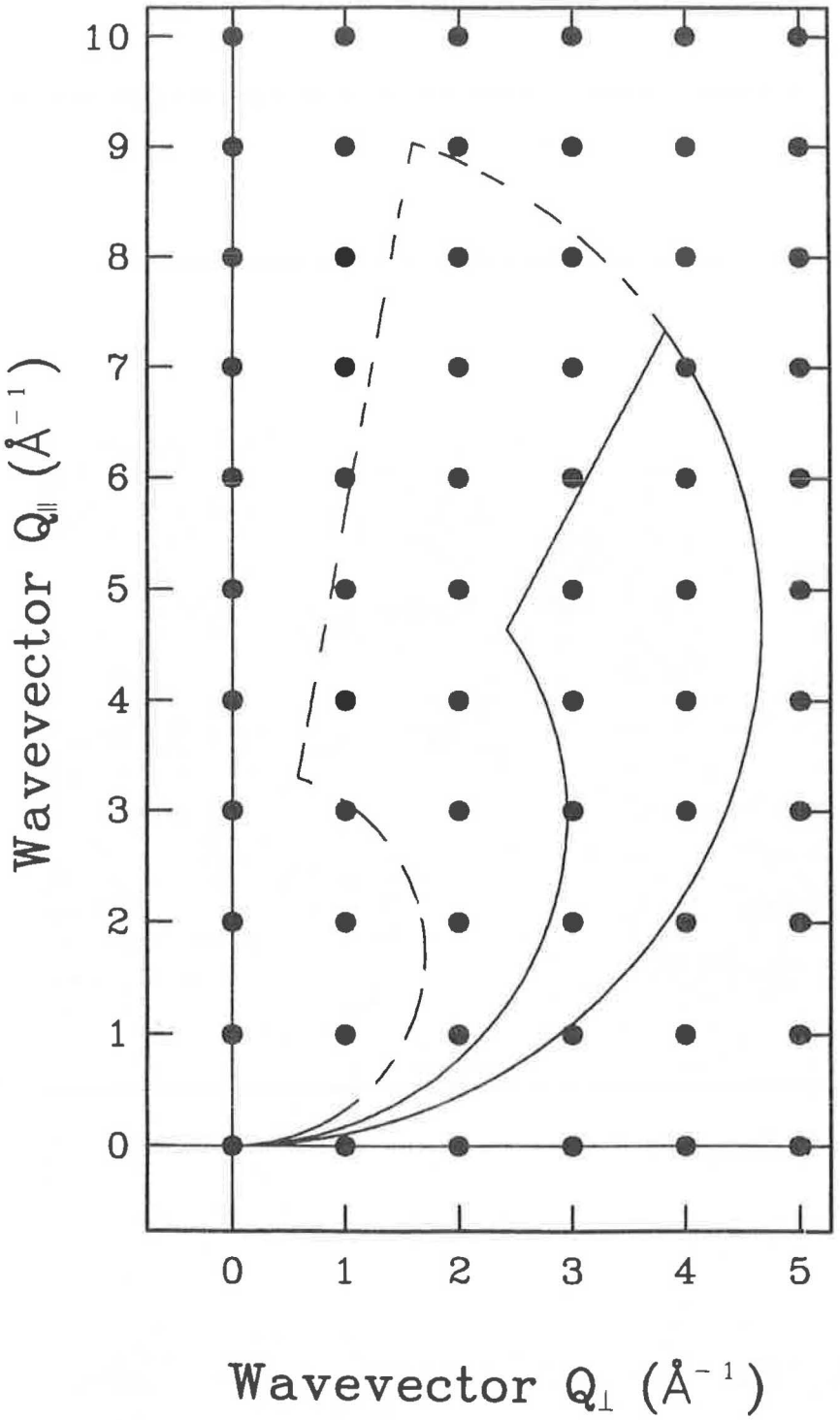
10
9
8
7
6
5
4
3
2
1
0
Wavevector $Q_{\parallel}$ ($Å^{-1}$)
0
1
2
3
4
5
Wavevector $Q_{\perp}$ ($Å^{-1}$)

Fig. 9